THE JOURNAL OF COMPARATIVE NEUROLOGY 498:649–666 (2006)

Long-Range Interneurons Within the Medial Pulvinar Nucleus of Macaque Monkeys

KOSUKE IMURA AND KATHLEEN S. ROCKLAND*
Laboratory for Cortical Organization and Systematics, RIKEN Brain Science Institute, Saitama 351-0198, Japan

ABSTRACT

ABSTRACT: Like other thalamic nuclei, the primate pulvinar is considered not to have long-range intrinsic connections, either excitatory or inhibitory. Injections of biotinylated dextran amine (BDA) in the medial pulvinar, however, reveal retrogradely filled neurons up to 2.0 mm from the injection edge. Serial section reconstruction (n = 18) confirmed that retrogradely filled neurons projected to the injection site and showed that they had additional long-range collaterals within the posterior pulvinar. Arrays of small, beaded terminations occurred in multiple foci along the collaterals. Terminal arrays were up to 1.0 mm in length; foci were separated by about 0.7 mm. Somata were large (average area = 220 μm^2), and dendritic arbors were radiate and also large (about 1.0 mm in diameter), but without either the appendages of classical interneurons or the hairlike spines characteristic of radiate pulvinocortical projection neurons. Double labeling for BDA and parvalbumin (PV) or BDA and γ-aminobutyric acid (GABA) indicated that these large neurons were positive for both PV and GABA. Double labeling for PV and GABA, or PV and glutamic acid decarboxylase 67 (GAD67) revealed a small number of similarly large neurons in the posterior pulvinar that were positive for both substances. Thus, we propose that these neurons are a novel class of inhibitory interneuron, longer range than the classic thalamic local circuit interneurons. Future questions include how these neurons relate to other inhibitory systems and specific postsynaptic populations and whether they are located preferentially within the posterior pulvinar, possibly related to the multimodal character of this thalamic region. J. Comp. Neurol. 498:649–666, 2006.

Indexing terms: axon collaterals; biotinylated dextran amine; divergence; inhibition; intrathalamic

On the basis of neurochemical and connectional features, recent studies have demonstrated finer subdivisions within the classical boundaries of the inferior, lateral, and medial pulvinar thalamic nuclei (reviewed in Gutierrez et al., 2000; Soares et al., 2001; Stepniewska, 2004). The micro-organization within and between these zones, however, remains poorly understood, as does the degree of perceptual transmission vs. higher order integration of information through the thalamus (Chalupa, 1991; Benevento and Port, 1995; Guillery, 1995, 2005; Grieve et al., 2000; Casanova et al., 2001; Sherman and Guillery, 2001, 2004; Basso et al., 2005; Shaman, 2005). Tracer injections in cortical areas show complex patterns of patchy anterograde and retrograde labeling, which do not completely overlap (e.g., Rockland, 1996; Steriade et al., 1997; Darian-Smith et al., 1999; Guillery et al., 2001; Taktakishvili et al., 2002; Baldauf et al., 2005a). This might indicate a mosaic or modular organization within the pulvinar, with local patches of pulvinocortical (PC) projection neurons and CP terminations (Shipp, 2003). Moreover, the pattern of different types of corticopulvinar (CP) terminations is by itself complex. Large cortical injections of anterograde tracers commonly result in convergent patches of type 1, small bouton projections; isolated or less convergent patches of type 2, large bouton arbors;

Grant sponsor: the RIKEN Brain Science Institute.

*Correspondence to: Kathleen S. Rockland, Ph.D., Laboratory for Cortical Organization and Systematics, RIKEN Brain Science Institute, 2-1 Hirosawa, Wako-shi, Saitama 351-0198, Japan.

E-mail: rockland@brain.riken.jp

Received 19 August 2005; Revised 12 December 2006; Accepted 29 April 2006

DOI 10.1002/cne.21085

Published online in Wiley InterScience (www.interscience.wiley.com).

as well as intermingled patches with both type 1 and type 2 projections (Rockland, 1996; Darian-Smith et al., 1999; Guillery et al., 2001; Taktakishvili et al., 2002; Baldauf et al., 2005a).

Consistent with a predominantly local or mosaic organization is the lack of long-distance intrinsic connections, from either inhibitory interneurons or from collaterals of PC projection neurons (Steriade et al., 1997; Sherman and Guillery, 2001, 2004). At least two features, however, are puzzling in the context of a strictly local architecture. These both relate to the configuration of CP projections. First, the typically sparse distribution of type 2 CP arbors seems insufficient to achieve coverage even of the smaller pulvinar subdivisions (Rockland, 1996; Steriade et al., 1997; Guillery et al., 2001). Second, single axon analysis shows that type 1 axons are, in contrast, typically branched and highly divergent, to the extent that they can easily be shown to cross over subdivisions (Figs. 10, 12, 13, and 19 in Rockland, 1996). Type 1 and type 2 terminations appear to originate from neurons in different cortical layers (respectively, from smaller neurons in layer 6 or from large neurons in layer 5; Steriade et al., 1997; Rouiller and Welker, 2000; Sherman and Guillery, 2001, 2004; Jones, 2002), and one commentary has even concluded, "It is possible that the microtopography of each [cortical] layer's projections differs in detail" (Shipp, 2003).

For the posterior portion of the medial pulvinar (PM), rather fewer data are available than for the retinotopically organized inferior and lateral subdivisions (Cusick et al., 1993; Gutierrez et al., 1995, 2000; Stepniewska and Kaas, 1997; Gray et al., 1999; Adam et al., 2000). At a global level, the PM has recently been subdivided into medial and lateral components, a laterally adjoining region (lateral dorsal pulvinar; PLd), and, except for the posteriormost levels, a ventrally adjoining part of the inferior pulvinar (PI; reviewed in Gutierrez et al., 2000; Soares et al., 2001; Stepniewska, 2004). In general, the PM receives connections from visual, auditory, and multimodal cortices.

Here, we report that injections of biotinylated dextran amine (BDA) in the posterior third of the PM result in retrogradely filled neurons up to 2.0 mm from the edge of the injection. BDA is an anterograde tracer, but it can produce retrograde labeling as well (see Materials and Methods). By serial section reconstruction of well-filled neurons, we corroborated that the neurons projected to the injection site and further ascertained that they had widespread collaterals. Subsequent combined immunohistochemistry indicated that BDA-labeled neurons were positive for parvalbumin (PV) and γ-aminobutyric acid (GABA). Further, double immunolabeling in separate experiments revealed a population of large neurons that were positive for both PV and glutamic acid decarboxylase 67 (GAD67). These were preferentially distributed in the posterior pulvinar, similar to the BDA-labeled neurons. From these two results, we propose that these neurons are a novel class of inhibitory interneuron in the posterior pulvinar. Because the collaterals extend well beyond the vicinity of the cell body, we have called these *long-range* interneurons, to distinguish them from classical thalamic local circuit neurons.

MATERIALS AND METHODS

Nine macaque monkeys (*Macaca mulatta* and *Macaca fuscata*, 4.2–5.8kg) of both sexes were used in the present study. Five monkeys were used for tracing studies, in which BDA was injected into the posterior part of the PM. In a sixth monkey, wheat germ agglutinin-horseradish peroxidase (WGA-HRP) was injected into parietal area 7. In three of these six animals, double staining was carried out for tracer (BDA or WGA-HRP) and PV or GABA. Three additional brains were used only for single or double immunohistochemistry, for PV and GABA, or PV and GAD67. This research was performed under guidelines of the official Japanese regulations for research on animals, according to institutionally approved protocols (RIKEN Brain Science Institute, Japan) and in accordance with the U.S. National Institutes of Health *Guide for the Care and Use of Laboratory Animals* (NIH Publication No. 80-23, revised 1996).

Surgery

Surgery was carried out under sterile conditions after the animals were deeply anesthetized with barbiturate anesthesia (35 mg/kg Nembutal i.p., following a tranquilizing dose of 11 mg/kg i.m.). First, a small craniotomy (5–10 mm) was opened contralateral to the injection target, in a dorsal position approximately overlying the posterior pulvinar, as estimated by stereotaxic coordinates (Paxinos et al., 2000). This was to permit online ultrasound imaging (LOGIQ9, GE Medical Systems, Milwaukee, WI; Tokuno et al., 2002) of the posterior region of the pulvinar. For maximum resolution, this was imaged contralaterally, typically in relation to the superior colliculi, which were clearly visible. Then, a second craniotomy was opened over the injection target; and a filled Hamilton syringe (10 μl), coated with Teflon spray (New TFE coat, Finechemical Japan, Tokyo, Japan) was lowered into the pulvinar under ultrasound visualization. For one monkey, magnetic resonance (MR) images were obtained preoperatively and used in conjunction with stereotaxic coordinates and ultrasound visualization to guide in the accurate localization. Five monkeys received one (n = 3) or two (n = 2) injections of 10% BDA (0.5–1.5 μl; 1:1 mixture of 3,000 and 10,000 MW, in 0.0125 M phosphate-buffered saline (PBS; pH 7.4); Molecular Probes, Eugene, OR) into the PM. For one monkey, 5% WGA-HRP (1.0 μl in 0.1 M PBS, pH 7.4; Toyobo, Osaka, Japan) was injected into parietal area 7 to label pulvinocortical projection neurons retrogradely. Area 7 was identified by direct visualization, after a craniotomy and duratomy, in relation to sulcal landmarks (i.e., intraparietal and superior temporal sulci).

Fixation and tissue preparation

After 14–21 days (for BDA) or 2 days (for WGA-HRP) postinjection survival, the monkeys were reanesthetized by an overdose of Nembutal (75 mg/kg) and transcardially perfused, in series, with saline containing 0.5% sodium nitrite (0.3–0.5 liter), 4% paraformaldehyde (4 liters, in 0.1 M phosphate buffer [PB], pH 7.4), and 0.1 M PB containing sucrose (0.5 liter each of: 10, 20, and 30%). Cerebral hemispheres were separated, further trimmed as two large blocks, and immersed in 30% sucrose in 0.1 PB for cryoprotection for 2–3 days at 4°C. Brain blocks were cut coronally using a freezing microtome, at 50 μm thickness, and tissue sections were collected in an uninterrupted series for BDA or a repeating series in the case of additional procedures (see below).

Single staining for BDA by diaminobenzidine

For three brains (R78, R81, and 292), sections were washed with 0.1 M PB containing 0.5% Triton-X-100 and reacted with a solution of avidin-biotin complex labeled with horseradish peroxidase (1 drop of reagent per 7 ml of 0.1 M PBS, pH 7.4; ABC Elite kits, Vector, Burlingame, CA), overnight at room temperature. After washes in 0.1 M PB, the sections were reacted with diaminobenzidine (DAB) containing 0.5% nickel ammonium sulfate.

BDA was first introduced as primarily an anterograde tracer (Brandt and Apkarian, 1992; Veenman et al., 1992). However, in some pathways, some amount of retrograde transport can occur ("BDA gives a capricious retrograde labeling," Vercelli et al., 2000). According to some reports, low molecular weight BDA (3,000 MW) favors retrograde labeling, whereas high molecular weight BDA (10,000 MW) favors anterograde labeling (Reiner et al., 2000; Product Information, Molecular Probes). On the basis of our previous experiences with BDA, we would agree that it is "capricious" as a retrograde tracer. Thus, although we consistently observed retrograde labeling in the vicinity of the five pulvinar injections, quantification about neuron distribution must be viewed with caution, and the possibility of false negatives cannot be ruled out.

Double immunofluorescence staining for BDA and PV, and BDA and GABA

In two other brains (299 and 310), we investigated whether retrogradely labeled BDA neurons in the pulvinar were positive for PV (PV+) or GABA (GABA+). A repeating series of three sections was prepared. One of these was reacted for BDA with DAB, as above. The other two were processed for double fluorescent labeling with BDA and PV, or BDA and GABA. Sections were immunoblocked in blocking solution (0.1 M PBS containing 0.5% Triton-X-100 and 5% normal goat serum) for 1 hour at room temperature and subsequently incubated with mouse monoclonal anti-PV antibody (1:5,000; Swant, Bellinzona, Switzerland; cat. no. 235) or rabbit polyclonal anti-GABA antibody (1:500; Sigma, St. Louis, MO; cat. no. A2052) for 2 days at 4°C. After washing with 0.1 M PBS, the sections were further processed to visualize BDA by fluorescence. For this, sections were incubated for 1.5 hours at room temperature in a mixture of Alexa Fluor 594-conjugated streptavidin (st-avidin, 1:200; Molecular Probes), and secondary antibodies Alexa Fluor 488-conjugated anti-mouse *or* Alexa Fluor 488-conjugated anti-rabbit polyclonal goat antibody (1:200; Molecular Probes). After analysis and photographic documentation of labeled cells, the fluorescent sections were further reacted in ABC and DAB. This achieved a permanent record of the BDA-labeled cells and, more particularly, filled in the gaps in the BDA series, so that serial axon reconstruction could be carried out. (The fluorescent signals for PV and GABA were lost in this final step.)

Double immunofluorescence staining for WGA-HRP and GABA, PV and GABA, and PV and GAD67

In one brain (298), sections were divided into two series. To visualize GABA immunoreactivity and WGA-HRP labeling together, one series of sections was incubated in primary antibody for GABA (as above), and then the sections were further reacted, for 20 minutes at room temperature, in a biotinylated Tyramide Signal Amplification solution (1:100; TSA Individual Reagent Pack, PerkinElmer, Boston, MA) for WGA-HRP detection. After washing with 0.1 M PBS, sections were incubated in ABC solution for 1.5 hours at room temperature, followed by a mixture of secondary antibody for GABA and Alexa Fluor 594-conjugated st-avidin for another 1.5 hours (1:200). The second series of sections was reacted for double immunofluorescence for PV and GABA. The sections were incubated in a mixture of primary antibodies for PV and GABA after blocking, and label was then visualized by Alexa Fluor-conjugated secondary antibodies (see above).

In another brain (287), sections were incubated in a mixture of rabbit polyclonal anti-PV antibody (1:500; Swant; cat. no. PV-28) and mouse monoclonal anti-GAD67 antibody (1:500; Chemicon, Temecula, CA; cat. no. MAB5406) after blocking; label was then visualized by Alexa Fluor-conjugated secondary anti-rabbit or anti-mouse antibodies, respectively (as above).

Single immunoperoxidase staining for PV or GAD67

In one brain (R74), sections were immersed in blocking solution and then incubated with mouse monoclonal anti-PV primary antibody (1:50000; Swant) for 2 days at 4°C. Finally, sections were incubated with biotinylated anti-mouse secondary antibody (1:200; Vector), and visualized by ABC and DAB. In addition, in brain R94, sections were collected in two alternating series and processed either for GAD67 alone or double immunoreacted for PV and GAD67 (described in the next section). For the single reaction, sections were immersed in blocking solution, incubated with mouse monoclonal anti-GAD67 primary antibody (1:5,000; Chemicon) for 2 days at 4°C, incubated with biotinylated anti-mouse secondary antibody (1:200; Vector), and visualized by ABC and DAB.

Double immunoperoxidase staining for PV and GAD67

Sections were incubated with mouse monoclonal anti-GAD67 primary antibody (1:5,000; Chemicon), after blocking for 2 days at 4°C. Then sections were incubated with biotinylated anti-mouse secondary antibody (1:200; Vector) and visualized by ABC and DAB with 0.5% nickel ammonium sulfate. The sections were incubated again with rabbit polyclonal anti-PV primary antibody (1:3000; Swant) overnight at room temperature. Then sections were incubated with biotinylated anti-rabbit antibody (1:200; Vector) and visualized by ABC and DAB without nickel ammonium sulfate.

Further antibody description

The PV antibody used here has been described in Celio et al. (1988). According to technical information by the manufacturer (Swant), it specifically stains the ^{45}Ca-binding spot of parvalbumin (MW 12,000 and IEF 4.9) in a two-dimensional immunoblot. For the GABA antibody, the manufacturer's (Sigma) technical information reports positive binding with GABA and GABA-KLH in a dot blot assay and negative binding with bovine serum albumin. For the GAD67 antibody, the manufacturer's (Chemicon) technical information reports no detectable cross-reactivity with GAD65 by Western blot analysis on rat brain lysate.

Routine controls for immunostaining were carried out in the course of these experiments, by omission of one of the primary antibodies. Controls have also been described in previous studies in primate, for example, Jones and Hendry, 1989 (parvalbumin in thalamus); Kultas-Ilinsky et al., 2004 (GABA in thalamus); or Levesque et al., 2004 (GAD67 in striatum).

Data analysis

Sections were scanned for well-filled retrogradely labeled neurons, in which the axon initial segment or proximal axon portion could be recognized. We sampled neurons that were located lateral and posterior to the injection sites, by at least 0.5 mm. By this procedure, we hoped to lessen the possibility that neurons might have been filled by their axons passing through the injection site, rather than by true retrograde transport from terminations at the injection site. Twenty neurons were analyzed for detailed dendritic morphology. For 18 of these, serial section reconstruction was carried out to map the axon configuration. Ten of these axons were mapped throughout several collaterals. Eight reconstructions were more limited but were mapped sufficiently beyond the first branch point to verify the long-range configuration. An additional five axon segments were partially reconstructed and shown to have the same branching pattern and terminal morphology, but these were not followed back to cells of origin.

For analysis of putative double labeling (BDA and PV, or BDA and GABA), we first obtained a photographic record of the fluorescent label. After completing the reaction for BDA-DAB, neurons were selected that were double labeled for both BDA and PV, or BDA and GABA, and their axonal field was reconstructed through serial sections by using a light microscope, with a camera lucida drawing apparatus (MH-3, Olympus, Tokyo, Japan). All photographs were taken as digital images (Axioskop 2 plus, Carl Zeiss, Jena, Germany). The images were merged and adjusted for contrast and/or brightness to match the real image, by using image software (Adobe Photoshop 7.0, Adobe, San Jose, CA).

Soma size was assessed by generating digital images (using a 40× objective) and tracing the soma outlines on the computer screen, using the computer mouse. The field size was about 350 × 250 μm, and three to four sections were used. These were from two animals, except for the WGA-HRP material, which was based on measurements from one animal. GAD+PV+ and GAD+ neurons were measured from material processed for either fluorescence or DAB immunostaining. BDA-labeled and GABA+ neurons were measured in DAB-reacted material. WGA-HRP-labeled and GABA+ neurons were measured in immunofluorescent material. Pixels in the selected area (i.e., individual somata) were analyzed by AxioVision 3.1 software (Carl Zeiss) and calculated as square microns. The calculated soma areas between two populations were compared statistically by the two-tailed t-test. To achieve significance, we collected 100 neurons for GAD+ and GAD+PV+. Because results were similar for samples of 100 or 50 neurons, we used 50 neurons for measurements of WGA-HRP projection neurons. For BDA-labeled neurons, we measured only those neurons that we could verify had widespread axon collaterals (n = 18).

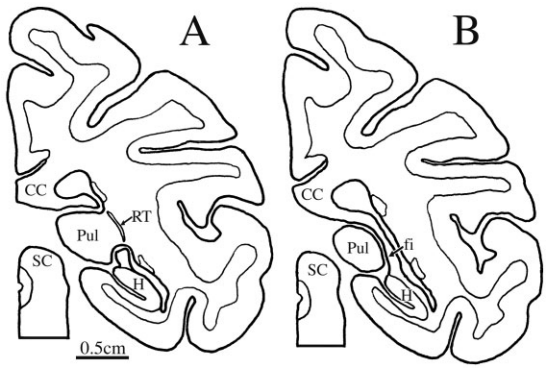

Fig. 1. Coronal section outlines (from case 292), corresponding to the photomicrographs in Figure 2A (section A) and D (section B). Section A is 0.4 mm anterior to section B. CC, corpus callosum; fi, fimbria; H, hippocampus; Pul, pulvinar; RT, reticular nucleus; SC, superior colliculus.

Nomenclature

The four classic subdivisions of the pulvinar nucleus (medial, lateral, inferior, and oral) have been intensively re-examined, especially in terms of neurochemical organization (Cusick et al., 1993; Gutierrez et al., 1995, 2000; Stepniewska and Kaas, 1997; Gray et al., 1999; Adams et al., 2000; Soares et al., 2001; Cola et al., 2005). These studies have led to re-evaluation and finer subdivision, which for the inferior pulvinar have been extensive. For the PM, previous work noted differences in levels of acetylcholinesterase (AChE; Lysakowsi et al., 1986; Cavada et al., 1995), and more recently, medial and lateral subdivisions have been proposed, whereby the medial part of the PM is distinguishable by lower levels of AChE and PV (Gutierrez et al., 2000; Stepniewska, 2004). At the level of the brachium of the superior colliculus, studies agree that the PM does not extend to the lateral edge of the nucleus but is adjoined by portions of the traditional lateral pulvinar (see, for example, Soares et al., 2001). At caudal levels, at least one study reports the termination of the lateral subdivision, on the basis of histochemical markers, so that the PM would be considered to extend to the lateral edge (Gutierrez et al., 2000).

In the present study, for ease of comparison, we have designated the likely PMm and PMl subdivisions (see Results). In this nomenclature, our injections would be mainly within the medial part of the PM or at the border between the PMm and PMl. We have indicated our general area of interest in Figure 1, and the axon trajectories are indicated on schematics of section outlines, to suggest possible correlation with these subdivisions. More exact correlation with finer subdivisions has not been possible because of the need to preserve uninterrupted serial sections for analysis of BDA-labeled profiles.

RESULTS

Retrogradely labeled neurons

Injections of BDA were made in the posterior PM, toward the medial portion (for representative injection, see Fig. 2A). All five injections resulted in retrogradely labeled neurons (Fig. 2). These were very dense in the immediate

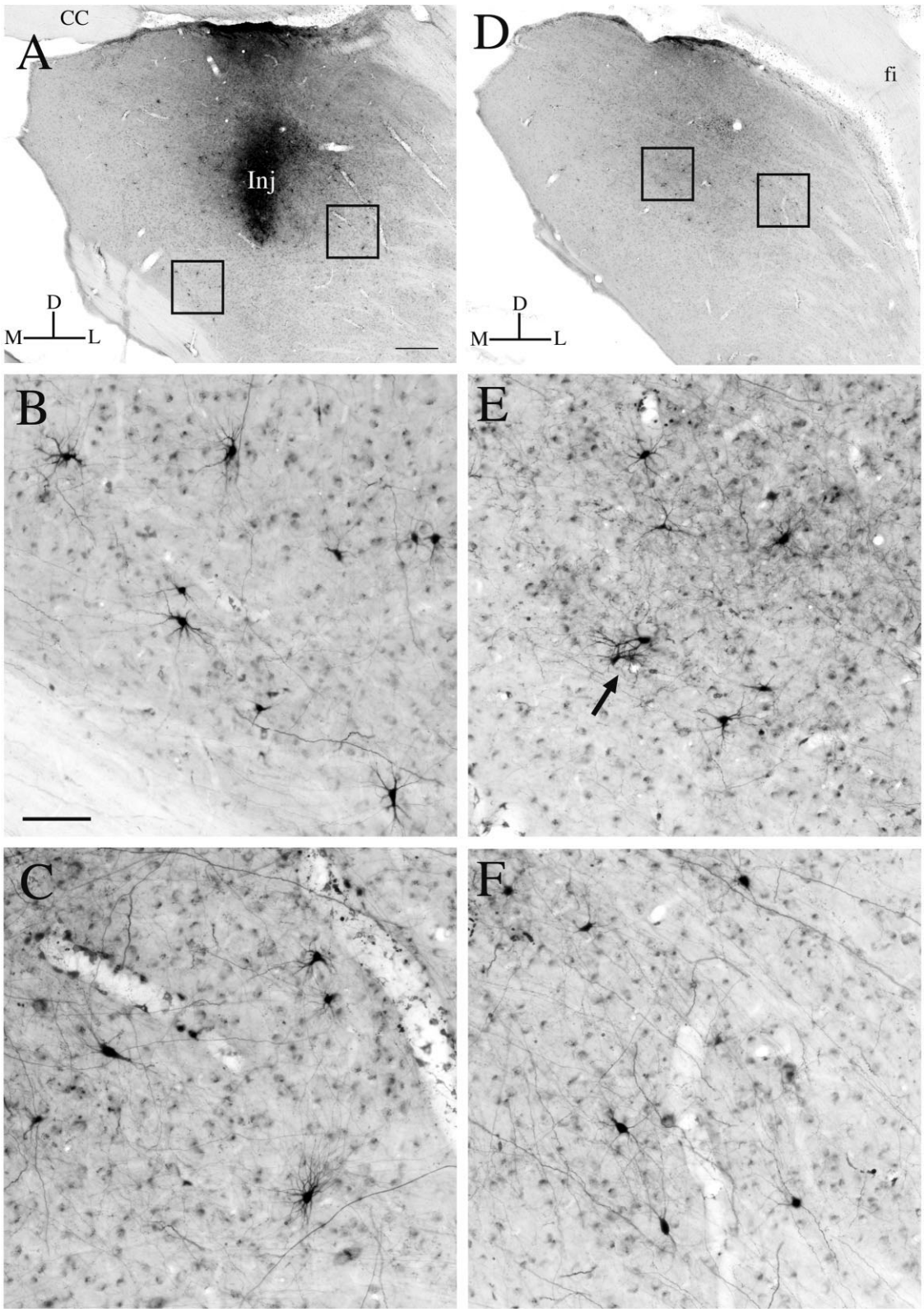

Fig. 2. Retrogradely labeled neurons in the medial pulvinar (PM) after an injection of BDA (case 292). **A:** Coronal section showing part of the injection site ("Inj."), and labeled neurons distributed 1.0–1.5 mm from the edge of the injection. **B,C:** Two boxed regions re-photographed at higher magnification, to show detail. **D:** Coronal section 0.4 mm posterior to A, with numerous labeled neurons (see Fig. 1 for general orientation). **E,F:** Two boxed regions re-photographed at higher magnification. Arrow in E points to small cluster of three labeled neurons. CC, corpus callosum; fi, fimbria; D, dorsal; L, lateral; M, medial. Scale bar in B = 500 μm for A,D; 100μm for B–F.

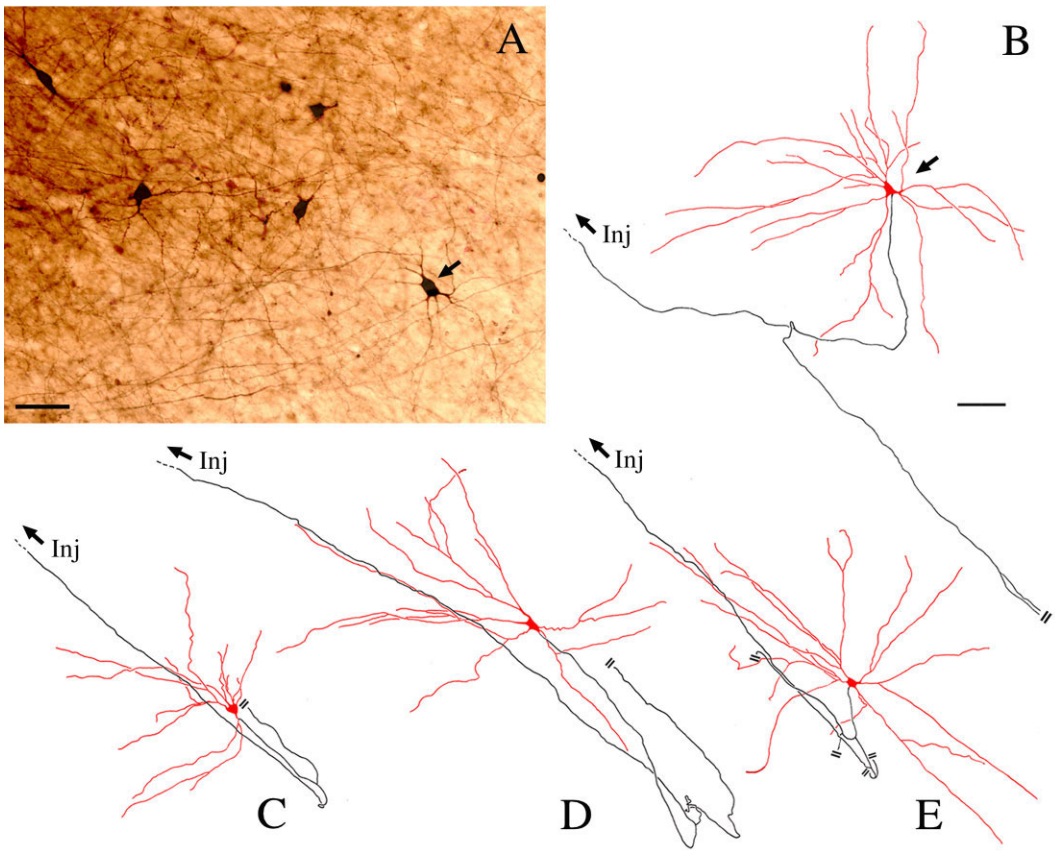

Fig. 3. **A:** Five retrogradely filled neurons in the PM, 1.1 mm lateral to the edge of the injection (case 292). Neuron at arrow is reconstructed through 26 sections, as illustrated in B. **B:** A typical long-range interneuron, with radiate dendritic morphology. (Soma and dendrites are in red.) The proximal portion of the axon is shown in black. **C–E:** Three additional reconstructions of similar neurons with radiate dendritic field (in red) and extended axon (in black). All four axons had one collateral that traveled dorsomedially to the injection site ("Inj" and arrow). Other collaterals were only partly analyzed. Short double lines here and in subsequent figures indicate partial reconstruction. Scale bar = 100 μm in A; 50 μm in B (applies to B–E). [Color figure can be viewed in the online issue, which is available at www.interscience.wiley.com.]

vicinity of the injection (within ~0.5 mm from the edge of the injections) but continued at lower density up to 2.0 mm away from the injection.

Clusters of three to five retrogradely labeled neurons were easily discerned (Figs. 2E, 7), but neurons were typically solitary, spaced at intervals of 0.2–0.8 mm apart (Fig. 2). As an estimate of density, we counted all retrogradely filled neurons in seven sections from one monkey, in a zone extending 3.5mm lateral from the medial edge of the nucleus. This yielded an average of 38 neurons per section (range of 29–47).

Somas were variable in shape, being multipolar, oval, triangular, or polygonal. Soma size was large (short axis: 10–20 μm; long axis: 15–25 μm). This is larger than reported for classical interneurons but similar to the size of projection neurons (in Golgi-stained material: Ma et al., 1998; Darian-Smith et al., 1999; and see Fig. 14 and below). Commonly, the BDA labeling continued throughout the dendritic tree and was Golgi-like in detail. By serial section analysis, we could thus determine features of the dendritic arbors. These were overall radiate and measured 0.8–1.0 mm in diameter (Fig. 3). This morphology was distinct from the "bushy" shape of pulvinocortical projection neurons (Steriade et al., 1997; Ma et al., 1998; Darian-Smith et al., 1999; Sherman and Guillery, 2001, 2004). It partly resembled the radiate subtype of projection neurons, except that there was no evidence of the hair-like processes that are exhibited by radiate pulvinocortical projection neurons (Ogren and Hendrickson, 1979; Ma et al., 1998; Darian-Smith et al., 1999). We caution, however, that their apparent absence may be due to incomplete filling by the tracer, despite the dense, Golgi-like filling (Figs. 4, 7).

Axon reconstructions

Detailed reconstructions were carried out from three of the brains with BDA injections, to corroborate that the retrogradely filled neurons in fact projected to the injection sites and to investigate further collateralization. Ten of 18 reconstructions were judged relatively complete (see the five profiles illustrated in Figs. 5, 6, and 8). The axon arborizations shared several characteristic features. First, boutons tended to be absent in the immediate vicinity of the cell bodies and did not overlap with the dendritic arbor. Second, at least five to six axon collaterals could be distinguished. Third, an individual axon had both short

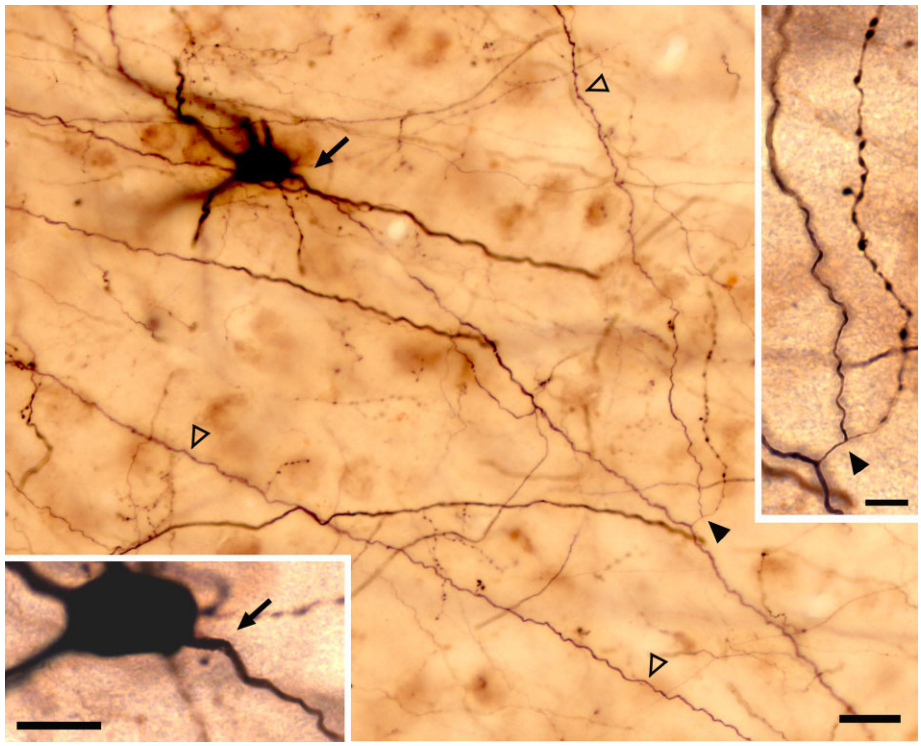

Fig. 4. Long-range interneuron in the PM retrogradely filled by BDA, with proximal portion of axon. One collateral with terminations (arrowhead) is shown at higher magnification in the right inset. The axon initial segment (arrow) is shown at higher magnification in the bottom inset. Hollow arrowheads mark more distal portions of the same axon. Other segments do not belong to this axon, as verified by serial section reconstruction (see Fig. 5). Scale bar = 20 μm; 5 μm in right inset; 10 μm in bottom inset.

(<0.5 mm) and longer (≥1.0 mm) collaterals. Fourth, terminal specializations were predominantly small and beaded and arranged in a rowlike fashion, without any well-defined arbors (Figs. 4–6, 8, 10). Fifth, there were multiple terminal foci, with some tendency for these to be spaced about 0.7 mm apart (center to center). The axons ramified over a territory of 1.0–2.0 mm^2 and <1.0 mm anterior-posterior, but no branches were found that extended laterally into the white matter beyond the pulvinar edge. Sixth, bouton numbers were relatively small, ranging from 150 to 600 per axon. Bouton density ranged from 44 to 69 boutons per 300 μm segment (samples taken from six segments, indicated by the six hollow arrowheads, of the axons in Figs. 5, 6, and 8). For the densest regions, the range was 18–25 boutons per 100 μm, which corresponds to an average interbouton interval of 5.0 μm. Together, these six features constitute a recognizable fingerprint. The eight partial reconstructions all conformed to some of these features, namely, the absence of boutons proximally, the occurrence of branches, and the small beaded shape of the terminations. Importantly, we remark that the spatially divergent collaterals are readily distinguishable from the dense local arborizations of classical intrinsic interneurons (Steriade et al., 1997; Ma et al., 1998; Sherman and Guillery, 2001, 2004).

Relation of reconstructions to pulvinar subdivisions

Four neurochemically distinct subdivisions have been distinguished within the dorsal pulvinar and have been described as maximally developed near the level of the brachium of the superior colliculus (Gutierrez et al., 2000; Soares et al., 2001; Stepniewska 2004). At more posterior levels, corresponding to our injection sites, the PM has been subdivided into medial and lateral sectors (PMm and PMl; see Nomenclature, above). By comparison with Gutierrez et al. (2000) and Stepniewska (2004), we can suggest that the cell body in Figure 5 is at the border of the two PM subdivisions; its three collaterals (1–3) appear to be within the PMm, but the more posterior collateral (4) may lie in the PMm or PMl. The cell bodies and collaterals of the two neurons in Figure 6A and B could all be at the border of the PMm and PMl. The cell body and collateral 1 of the neuron in Figure 6C both seem to be within the PMm, but the more posterior collateral 2 could be at its lateral border, and the cell body and three collaterals of the neuron in Figure 8 could all be at the border of the PMm and PMl. Inhomogeneities, possibly indicative of finer subdivisions, have been remarked in both the PMm and PMl (Gutierrez et al., 2000), but we have no grounds for determining whether the labeled cell bodies and/or their collaterals have any preference for these finer subdivisions.

Double immunofluorescence: BDA and GABA, BDA and PV, PV and GABA, and PV and GAD67

Because our axon reconstructions failed to reveal any axon branches beyond the pulvinar nucleus itself, we considered that these neurons might be a novel class of long-range interneuron. In order to distinguish more clearly

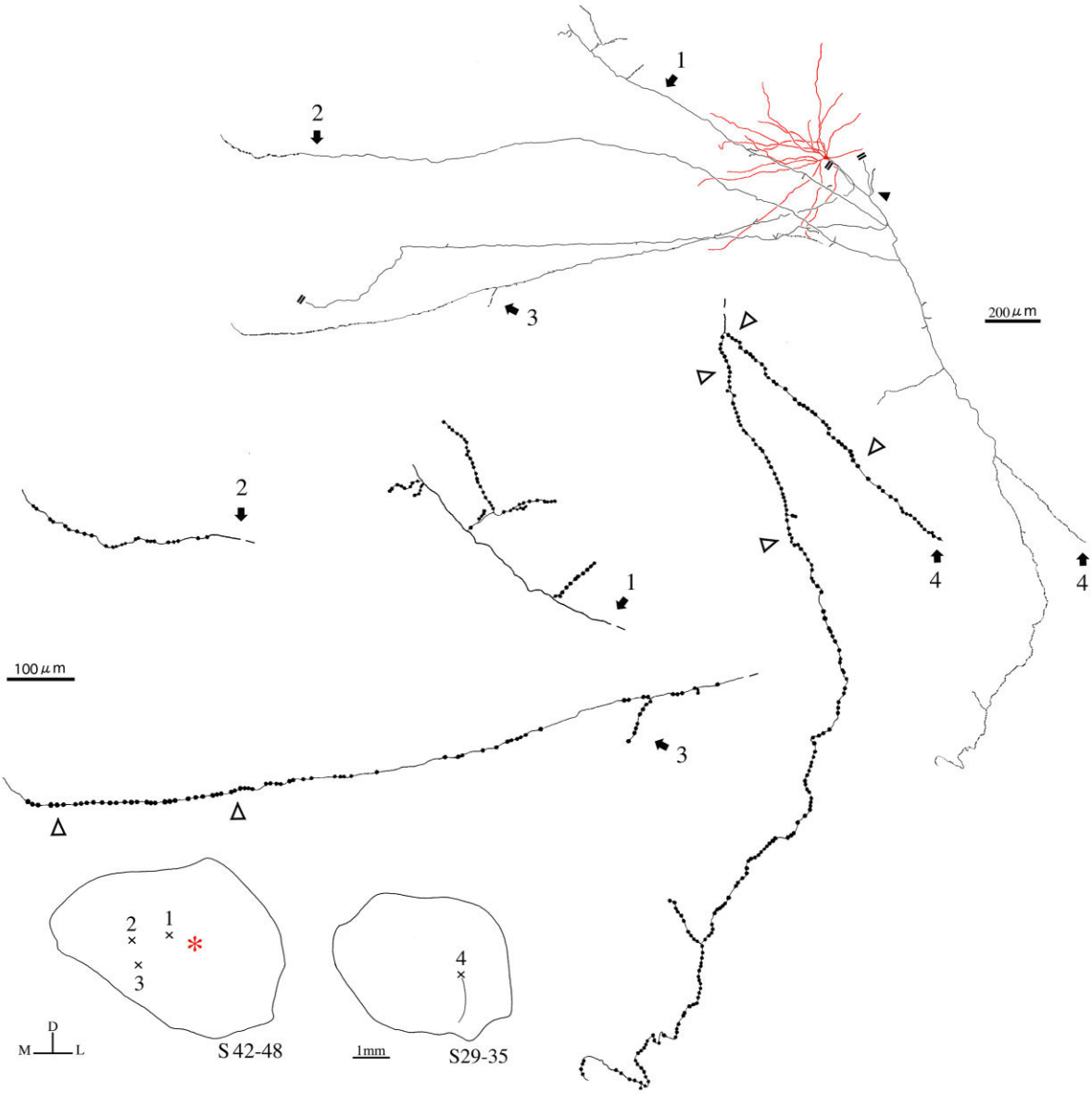

Fig. 5. Serial section reconstruction of the neuron illustrated in Figure 4. (Portion at arrowhead corresponds to the right inset in Fig. 4.) The axon has at least five major collaterals. Four of these (at numbered arrows) carry terminations and are redrawn at higher magnification to show detail. (Size of terminations is standardized, and slightly exaggerated for the sake of clarity.) The approximate location within the pulvinar of the four numbered segments is indicated by numbered X's on two schematic coronal outlines at bottom. The full extent of branch 4 is indicated by a line at the same scale as the section outlines, and the position of the cell body (2.7 mm lateral from the injection edge) is shown by the asterisk. Numbers below the schematics indicate merging of seven sections, and AP level, where smaller numbers are more posterior. The hollow arrowheads indicate three segments used to calculate bouton density and interbouton interval. The same conventions apply to Figures 6 and 8.

between possible projection neurons and interneurons, we proceeded to investigate the chemical properties of these neurons, by carrying out double staining in selected sections, for BDA and GABA, BDA and PV, PV and GABA, or PV and GAD67. For the two BDA groups, we imposed stringent criteria of soma size, Golgi-like filling, identifiable dendrites, and, in a final step after DAB processing, at least partial axon recovery. These criteria severely limited the number of neurons that we could evaluate for double labeling. For the two PV groups, we used the criteria of soma size and dense quality of filling into at least proximal dendrites. Results in tissue reacted for GABA or GAD67 were indistinguishable, and the term *GABAergic* will be used for both populations.

Double staining for BDA and GABA revealed nine neurons that were unambiguously double labeled. (Three of these are illustrated in Fig. 7.) After photographic documentation of the fluorescent label, the tissue was further reacted for BDA-DAB (Fig. 7D), and three of the nine BDA-GABAergic neurons were analyzed through

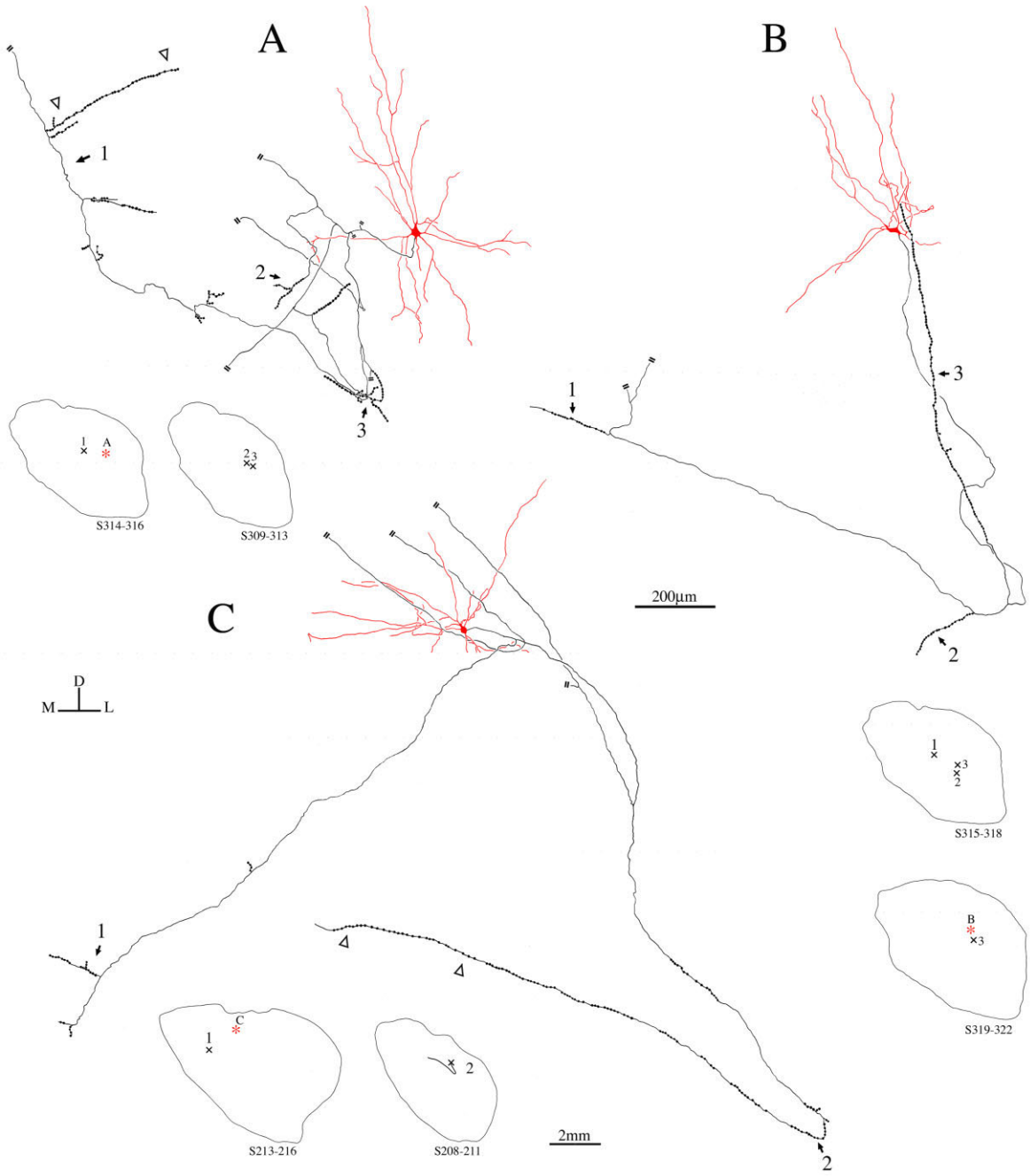

Fig. 6. Three additional reconstructions of long-range interneurons, with soma and dendrites (in red) and axon collaterals (in black). The approximate location of the numbered segments and cell bodies are depicted on the schematic outlines of the pulvinar by numbered X's (axon segments) and red asterisk (cell body).

serial sections. These were confirmed to have radiate dendritic morphology and an extended axonal arborization with multiple branches and small beaded terminations (Fig. 8).

After staining for BDA and PV, five neurons were determined to be double labeled. After a final DAB step, four of these were analyzed through serial sections and were found to have radiate dendritic morphology, extended axon arborization, and beaded terminations. Thus, we can conclude that at least some of the BDA-labeled neurons were positive for GABA or PV.

In the PM, projection neurons were PV+ and GABA−, but interneurons might be PV+ and GABA+. One study in the magnocellular medial geniculate nucleus has reported a population of large neurons positive for both GABA and PV (Jones and Hendry, 1989). In order to

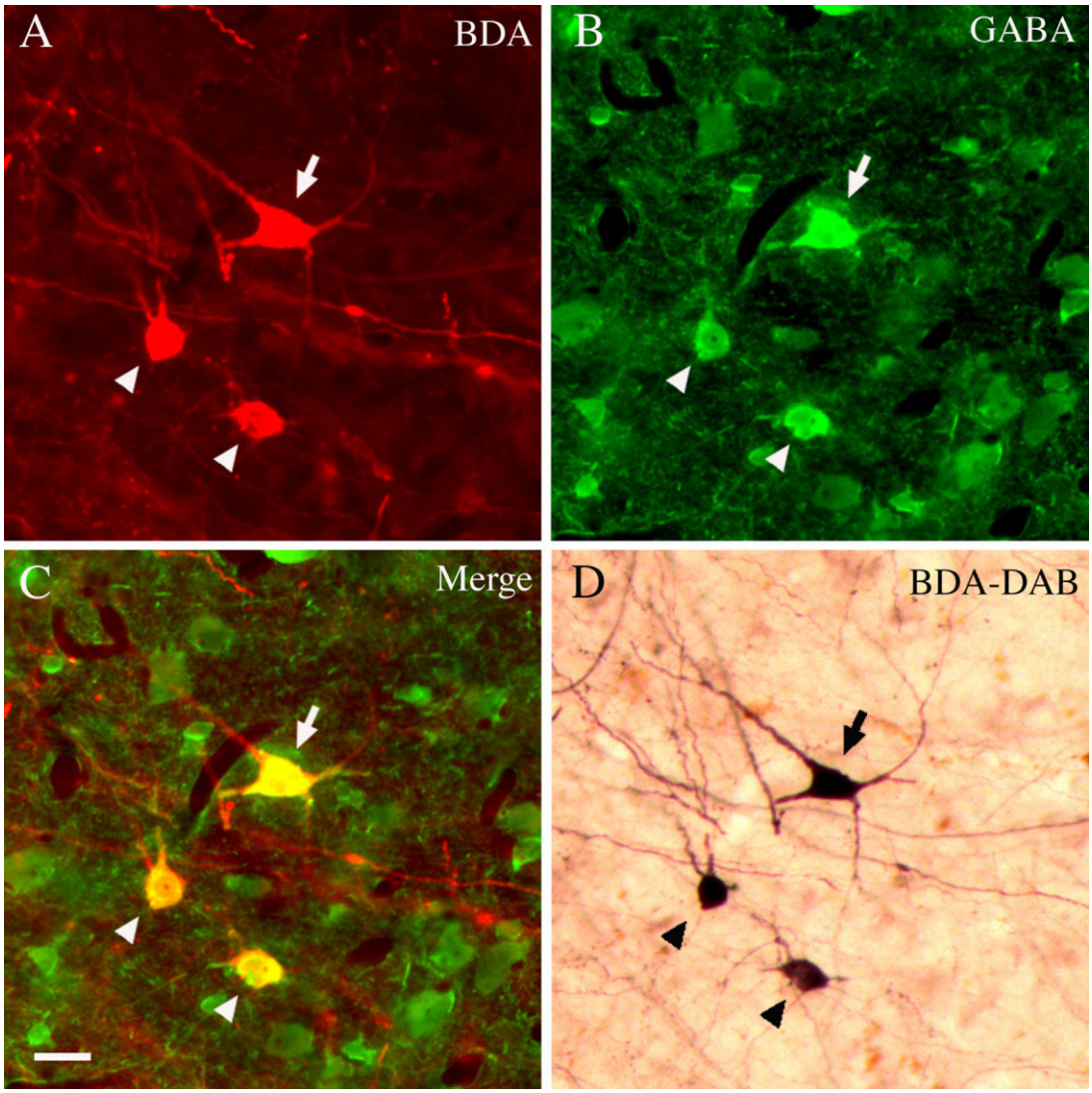

Fig. 7. Cluster of three neurons retrogradely labeled by a BDA injection in PM and double-labeled for GABA. **A:** Neurons are visualized by streptavidin-Alexa (in red). **B:** The same three neurons (arrow and arrowheads) are positive for GABA, as verified by the merged image in **C**. **D:** The same three neurons after subsequent reaction with ABC and DAB. This allows detailed axon reconstruction, which was carried out for two of these neurons (one of which, at arrow is shown in Fig. 8). Scale bar = 20 μm in C (applies to A–D).

determine whether the BDA+PV+ population might also be GABAergic, double staining for PV and GABA or GAD67 was carried out (Figs. 9, 11, 12). On the basis of cell size, neurons positive for GABA or GAD67 could be subdivided into two subpopulations, those with small (S.A.< 6 μm; L.A. < 12 μm) or large (S.A. > 12 μm; L.A. > 20 μm) soma. In all cases, the large GABAergic neurons co-localized with PV, and we thus propose the identification of these neurons as a novel class of long-range inhibitory interneuron.

In three sections from one monkey, we scored the distribution of large GAD+PV+ neurons (Fig. 13). Like the BDA-labeled neurons, these tended to be scattered, although occasional clusters of up to eight neurons also occurred. A very few neurons were detected in what could be the PIp (Fig. 13C) and PLd (Fig. 13B), but most were concentrated in subdivisions of the PM. Although this is consistent with the distribution of BDA-labeled neurons and the axon reconstructions at posterior levels, the GAD+PV+ neurons are only putatively long range, and we cannot be sure of that these two populations are identical.

Double immunofluorescence staining for GABA and WGA-HRP

Given our results, that the long-range interneurons are GABAergic, it seemed unlikely that there would be co-localization with pulvinocortical projection neurons, because these are known to be excitatory. To check this directly, we carried out double labeling for GABA and WGA-HRP, after an injection into the parietal cortex, area 7 in one monkey. The injection resulted in many retrogradely labeled pulvinocortical neurons in both the PM

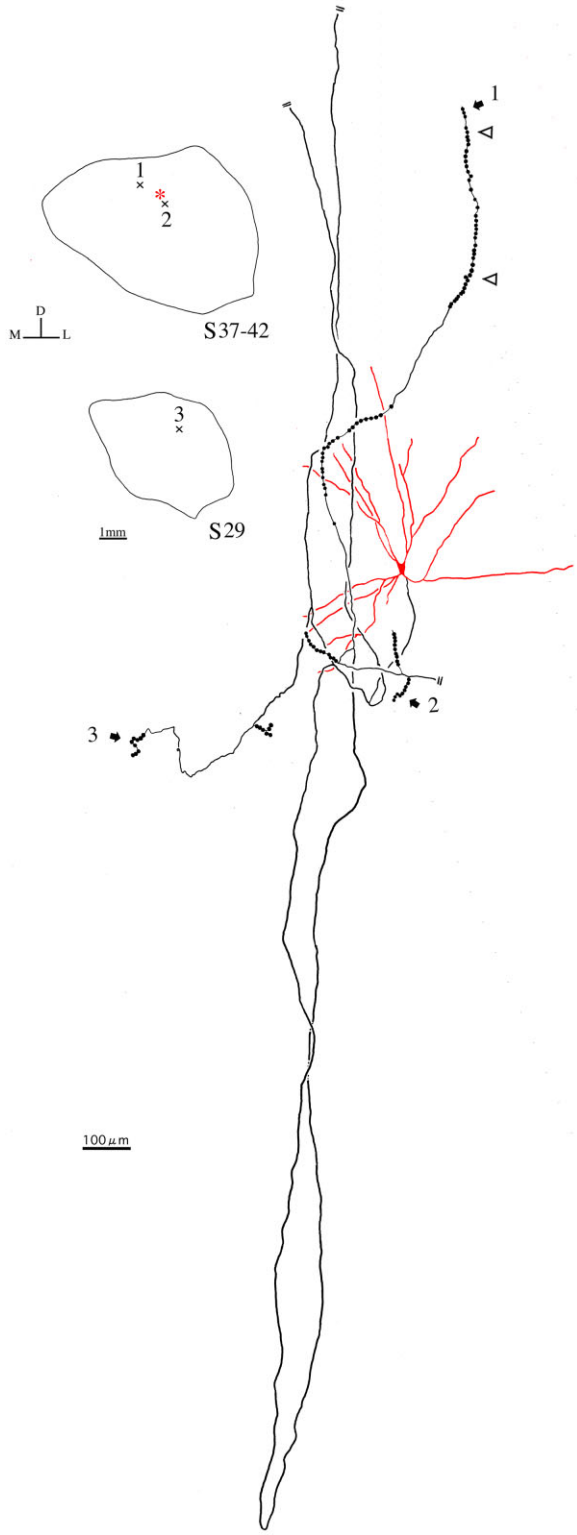

Fig. 8. Serial section reconstruction of one of the GABAergic neurons in Figure 7 (from arrow). There are six spatially separate groups of terminations, three of which are indicated by numbered arrows in the reconstruction and by numbered X's on the two schematics. The true orientation is closer to a 10:00–4:00 axis, but the image has been rotated here to conserve space.

and adjoining lateral pulvinar, as expected from previous studies (Baleydier and Mauguiere, 1987; Baleydier and Morel, 1992). Large and small GABAergic neurons intermingled with the field of WGA-HRP-labeled neurons, but none of the projection neurons were double labeled with GABA (Fig. 9E).

Immunostaining for PV

In the PM, what appeared to be at least two subgroups of PV+ neurons were readily distinguishable. The majority of PV+ cells were moderately stained, with little or no dendritic staining (Fig. 12). A smaller number, however, was densely stained in Golgi-like detail, through the dendritic arbor (Fig. 12). We would tentatively identify these densely stained PV+ neurons as long-range interneurons, as they have a similar dendritic morphology and soma size to the BDA-labeled population. Four partial reconstructions of neurons ascertained as double-labeled for BDA and PV support this identification (not illustrated). Because PV+ projection neurons are often large as well, a better criterion for identification of putative interneurons would be large neurons that are both PV+ and GAD67+.

In the PM, especially at the lateral edge of the nucleus, we could discern abundant small beaded terminations in the neuropil. Although these closely resembled the BDA-labeled terminations we have identified as belonging to long-range interneurons (Fig. 10), they could also derive from extrinsic sources. For example, neurons in the thalamic reticular nucleus (RTN) are known to be positive for PV (Jones and Hendry, 1989; Pinault, 2004), and BDA injections in the anterior part of RTN in the monkey reveal terminations that are small and beaded (Ilinsky et al., 1999).

Soma size of four neuronal populations

To verify our impression that long-range interneurons can be partly distinguished on the basis of large somas, we carried out a quantitative comparison of four populations. (Two are shown in Fig. 14.) First, in two monkeys we measured neurons (n = 100) that were GAD67+ but PV negative (GAD+PV−), as visualized by double immunofluorescence (Fig. 11; n = 19) or immunoperoxidase (Fig. 12; n = 81). The average soma area was small: 96 μm^2 in immunofluorescence and 103 μm^2 in immunoperoxidase. Second, in the same sections, we measured neurons (n = 100) double labeled for PV and GAD67. For these neurons, the average soma area was 231 μm^2 in fluorescent material (Fig. 11; n = 27) and 217 μm^2 in DAB-reacted material (Fig. 12; n = 73). Thus, the GAD67+PV+ population is significantly larger than the population of GAD67+/PV− neurons (two-tailed t-test; *, $P < 0.05$).

Two further comparisons were carried out on smaller populations. The average soma area of pulvinocortical projection neurons was 223 μm^2 (n = 50; WGA-HRP-labeled fluorescent material), which was not significantly different ($P > 0.05$) from that of GAD+PV+ neurons (Fig. 14B). Finally, the soma size was measured for 18 of the BDA-labeled neurons identified as long-range interneurons on the basis of full or partial axon reconstructions. The average size was 220 μm^2 (median = 209 μm^2), which is not statistically different ($P > 0.05$) from that of GAD67+PV+ neurons (217 μm^2 in DAB-reacted material). These results support our observations that long-range intrinsic neurons and neurons that are GAD67+PV+ have larger soma than classical interneurons.

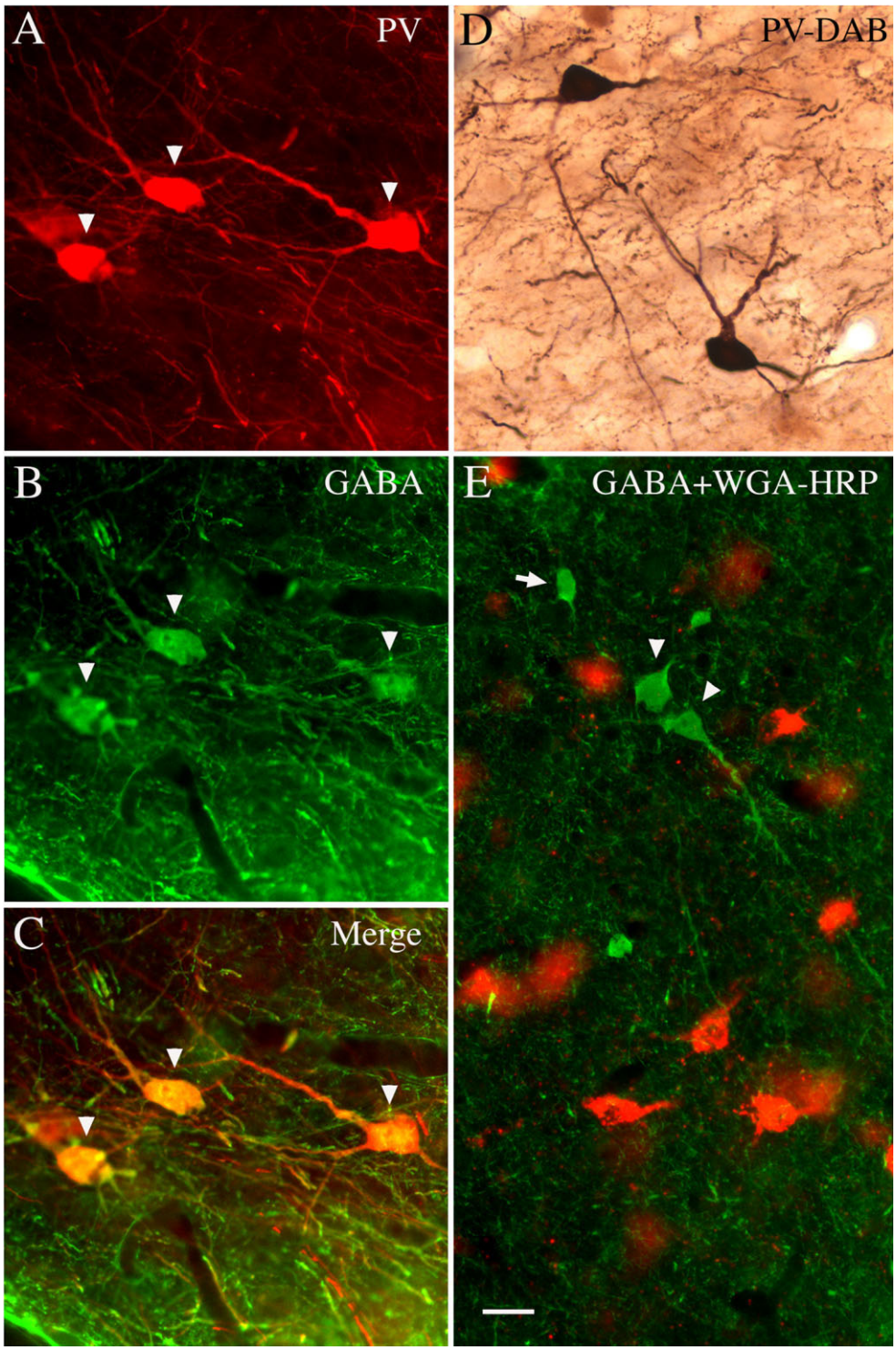

Fig. 9. Some PV+, putative long-range interneurons in the PM are also GABAergic. **A:** Three PV+ neurons (arrowheads; immunofluorescence). Note radiate dendritic morphology. **B:** The same three neurons (arrowheads) are GABAergic, as verified by the merged image in **C**. Soma size is larger than that of classical interneurons (see E). **D:** For comparison, a similar radiate dendritic morphology is demonstrated by PV-DAB immunocytochemistry. **E:** Pulvinocortical projection neurons (in red) do not co-localize with GABA. This field contains both small and larger GABAergic neurons (arrow and arrowheads, respectively; in green). Scale bar (in E) = 20 μm in E (applies to A–E).

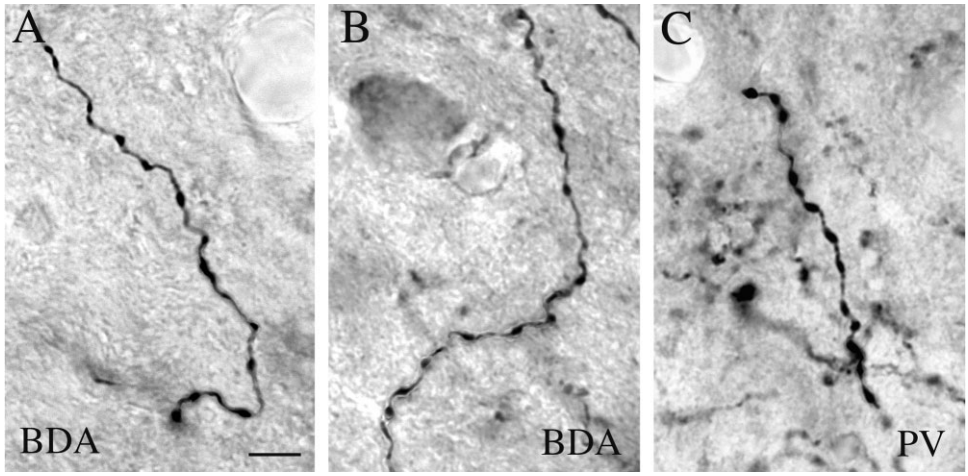

Fig. 10. **A,B:** Terminations of BDA retrogradely filled neurons are typically small and predominantly beaded (en passant). **C:** PV+ terminations in PM. Note similar morphology to BDA. Scale bar = 5 μm in A (applies to A–C).

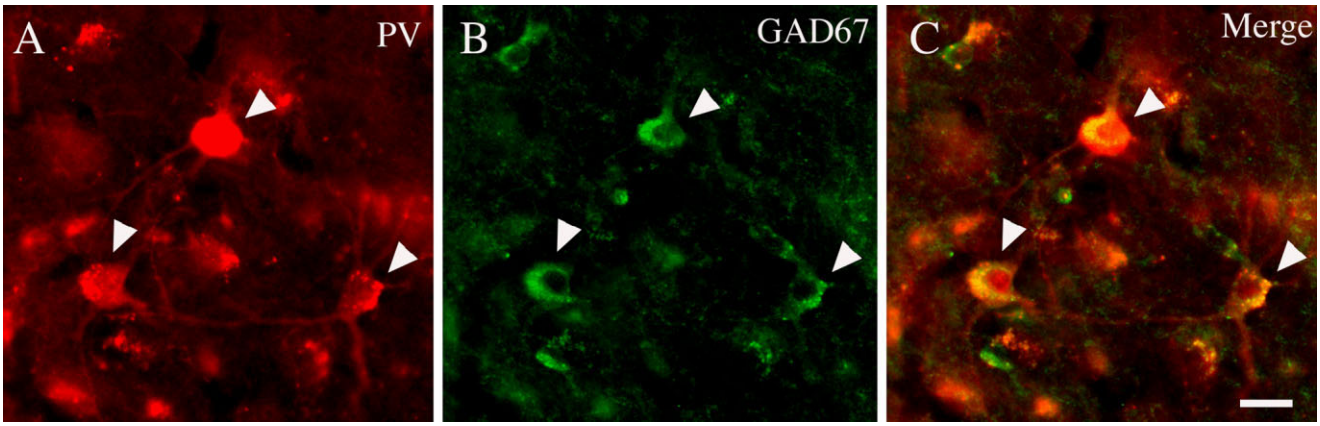

Fig. 11. Large PV+ neurons are positive for GAD67. **A:** A cluster of PV+ neurons in PM. Three large neurons are indicated by arrowheads. The same three neurons are positive for GAD67 (arrowheads in **B** and merged image, in **C**). Scale bar = 20 μm in C (applies to A–C).

DISCUSSION

In this report we present evidence that a subset of neurons in the posterior part of the pulvinar nucleus has a widespread axon collateralization extending at least 2.0 mm from the parent cell. This is based primarily on serial section analysis and tracing of the axons from retrogradely filled parent neurons. These neurons are characterized by large somata and a radiate dendritic tree, rather similar to one type of PC projection neuron. The identification of these neurons as interneurons and not projection neurons is supported by several observations. First, we were unable to find any collaterals that exited from the pulvinar in our reconstructions. Abundant fibers, presumably anterogradely labeled PC projecting axons, could be seen streaming laterally beyond the pulvinar, but these were not joined by any of the axons in our sample. Second, there are no reports from the monkey pulvinar nucleus that relay neurons have local collaterals, although we note that new reports have emerged noting that some relay neurons can have local collaterals, in the cat lateral geniculate nucleus (Cox et al., 2003) and rat paralaminar nuclei (Smith et al., 2006). Third, the radiate dendrites of PC projection neurons are reported to bear hairy appendages (Darian-Smith et al., 1999), but this was not the case for the long-range interneurons. Fourth, and importantly, the BDA-labeled neurons were positive for PV but also for GABA or GAD67. Large neurons, potentially the same as BDA-labeled neurons, were also identified as positive for GAD and PV and preferentially located in PM. Because part of the distal collateralization of our axon reconstructions is obscured within the injection sites, it is true that there could still be additional collaterals, including a PC branch that we missed. The neurons we analyzed, however, were either posterior or lateral to the injection, so that in the case of

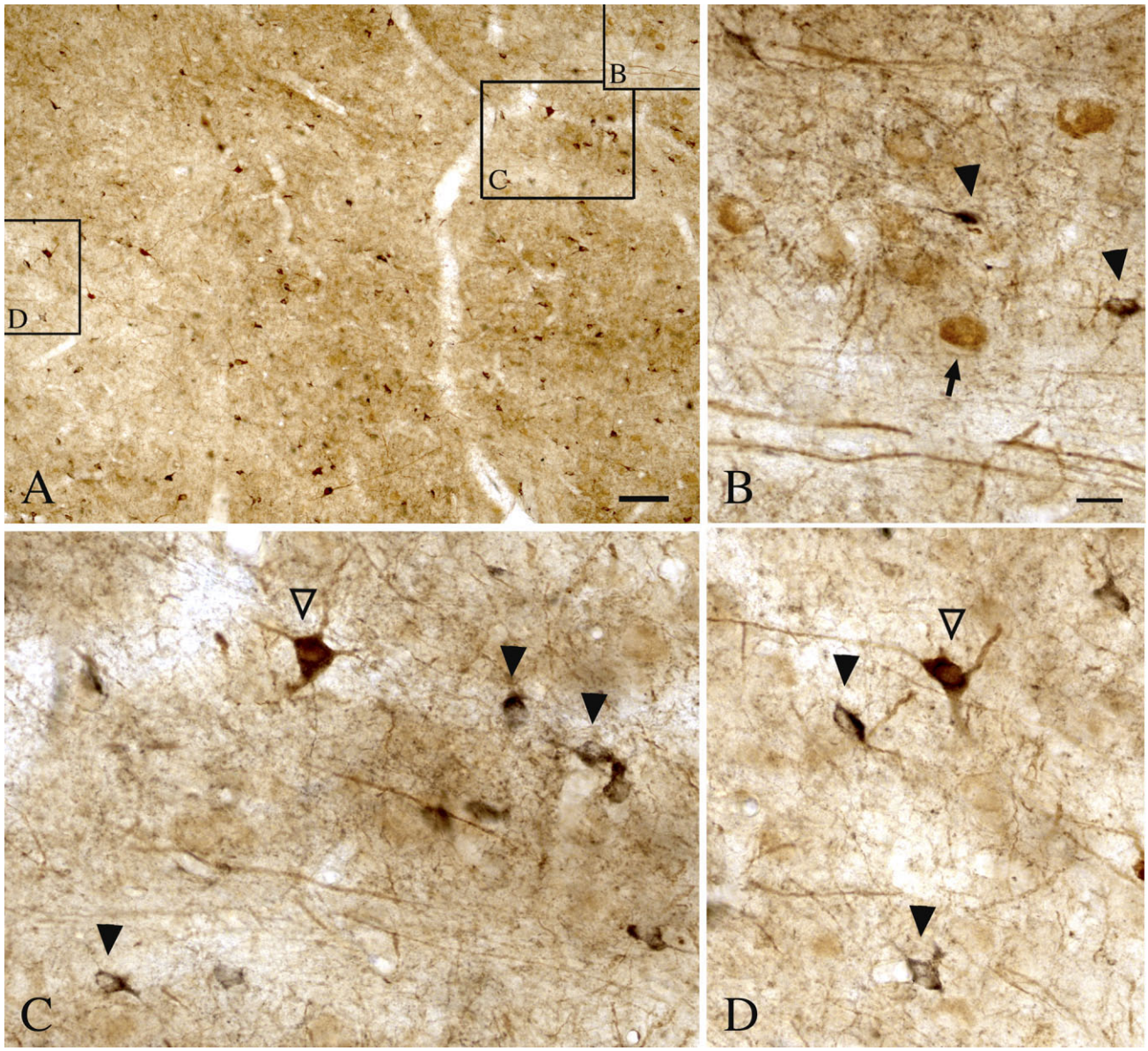

Fig. 12. **A:** Tissue double-reacted (with DAB and nickel-DAB immunoperoxidase) for PV (brown) and GAD67 (black). **A:** Low magnification of the border region between the PM (at left) and PL (at right). Three boxed regions are re-photographed at higher magnification in B–D. **B:** Large PV+ neurons (one of which is indicated by arrow), likely corresponding to pulvinocortical projection neurons. Two small, black GAD67+ interneurons are indicated by solid arrowheads. Note PV+ pulvinocortical fibers, characteristic of PL. **C:** One large neuron, PV+ and GAD67+ (at hollow arrowhead) and three small GAD+ interneurons (at solid arrowheads). **D:** One large neuron, PV+ and GAD67+ (hollow arrowhead) and a small GAD+ interneuron (solid arrowhead). Scale bar = 100 μm in A; 20 μm in B (applies to B–D).

an additional PC collateral, this would have to take an implausibly curved trajectory, detouring anteriorly and/or laterally through the injection site.

Several investigators have injected retrograde tracers into the medial pulvinar, without reporting retrogradely labeled neurons in the surround of the injection site. This is likely to be in part because of the diffuse halos associated with large injections of fluorescent dyes or HRP. In addition, without the control of axon reconstruction, retrogradely filled cell bodies might be interpreted as projection neurons labeled from axons damaged within the injection site or cut by the needle track.

Relationship with previous studies

Inhibitory interneurons make up about 30% of the neuronal population in the primate pulvinar and are known to be heterogeneous. The classical interneurons are GABAergic, with small somata and small dendritic arbors frequently bearing claw-like specializations that are presynaptic to other dendrites (Steriade et al., 1997; Sherman and Guillery, 2001, 2004). Their axons are very local in distribution and are obviously distinct from those of the long-range interneurons reported here. The Golgi literature, however, contains several reports of large local cir-

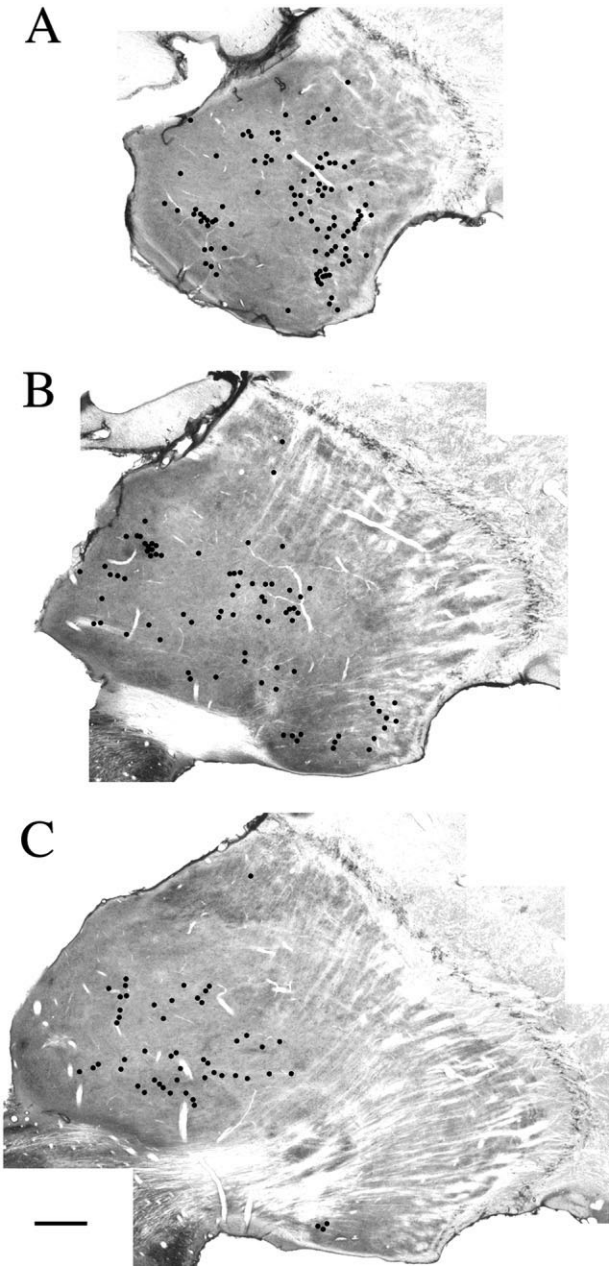

Fig. 13. Large neurons that are GAD+PV+ are shown as black dots in coronal sections at three different levels. **A:** Neurons are most numerous at the posterior level. **B,C:** Sections from progressively anterior levels. In C, a very few neurons were found in the PI, medially, and in what is probably the PLd, dorsolaterally. Scale bar = 1.0 mm in C (applies to A–C).

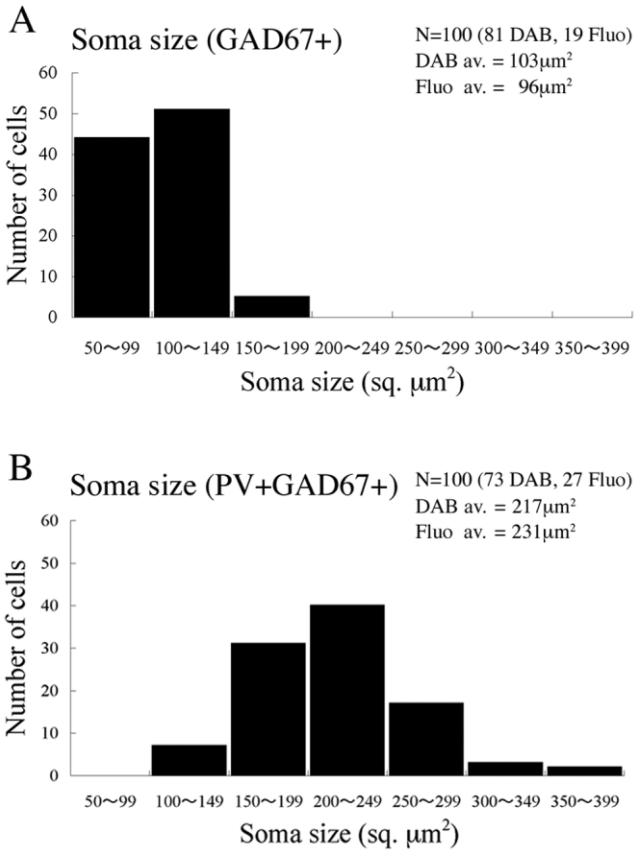

Fig. 14. Histograms illustrating the distribution of soma areas for two populations of neurons. **A:** GAD67+ interneurons. **B:** Neurons positive for both PV and GAD67. Neurons positive for both PV and GAD67 are proposed to be long-range interneurons. These have a significantly larger soma area than the subset that is only GAD67+. Fluo, immunofluorescent reacted material; a v., average soma area.

cuit neurons, which more closely resemble the BDA-labeled long-range interneurons. Tombol (1969) reported one subtype in the LGN in which the axon could be traced as far as 700–800 μm, although this was from a very young kitten (reviewed in Sherman and Guillery, 2001). Scheibel et al. (1972; their Fig. 7) illustrated a large "reticular-like" cell ("integrator") from the cat ventrobasal complex, with a bifurcating axon. Ogren and Hendrickson (1979; their Fig. 9) illustrated one neuron from the "border between inferior and lateral pulvinar," with a large soma and radiate dendrites. Like the neurons reported here, the axon is shown as branching in the vicinity of the cell body, is without boutons in its proximal portion, and extends for 250 μm before passing out of the section. One discrepancy, however, is that the dendrites terminate in specialized appendages, which were never seen in our material.

Studies in the rat (Gabbott and Bacon, 1994) and cat (Meng et al., 1996; Bickford et al., 1999) have described subsets of larger GABAergic interneurons that contain nitric oxide (NO) synthase; but the primate PM is almost entirely lacking in NO-positive neurons, as assayed by NADPH-diaphorase (personal observations, and Soares et al., 2001). GABAergic neurons have been previously described in the PM (Jones and Hendry, 1989; Hunt et al., 1991; and in squirrel monkey, Smith et al., 1987), without any size distinction. Large and small GABAergic neurons have, however, been reported in the dorsal division of the medial geniculate nucleus in cats (Huang et al., 1999). Clark et al. (1989) report that GABAergic neurons in the mediodorsal nucleus are slightly larger in the magnocellular portion, although the difference appears slight (mean diameter 10.4 ± 0.1 μm vs. 9.9 ± 0.1 μm).

Functional significance

Several recent investigations have revealed a diverse network of inhibitory inputs to higher order thalamic nuclei in rats. These originate from the zona incerta (Barth et al., 2002; Trageser and Keller, 2004; Mitrofanis, 2005) and from the anterior pretectal nucleus (APT; Bokor et al., 2005; and in cats: Baldauf et al., 2005b). In rats, the RTN is reported to mediate a network of intrathalamic connectivity (Crabtree and Isaac, 2002). In contrast to inputs from the RTN, those from the APT in rats target relay cells at the proximal dendritic region, have multiple release sites, and use only $GABA_A$ receptors, consistent with a fast phasic control of relay cell activity (Bokor et al., 2005). Although species differences are well known in the inhibitory thalamic systems (Arcelli et al., 1997), an interesting question is whether the functional characteristics of long-range interneurons might be more comparable to either the reticular or extrareticular sources of inhibition. There are several morphological points of similarity between long-range interneurons and RTN neurons, namely, both have large soma and large dendritic arbors, both have terminations that are small and beaded (Ilinsky et al., 1999), and, notably, both are GABAergic and PV+ (Jones and Hendry, 1989; Pinault, 2004). More data concerning the output targets and input connectivity of long-range interneurons might provide some clues. Although demonstration of these neurons on the basis of a widespread axonal arborization may be difficult, they can also be provisionally identified by the phenotype of large GAD+PV+ soma.

Another clue is the location of these interneurons, in the posterior part of the PM. From cortical tracer injections, we know that this region has widespread connections with the auditory association cortex, parahippocampal and orbitofrontal cortices, and parietal and temporal visual and multimodal areas (Baleydier and Mauguire, 1987; Baleydier and Morel, 1992; Baizer et al., 1993; reviewed in Robinson and Cowie, 1997; Gutierrez et al., 2000; Stepniewska, 2004). Most of our reconstructed axons preferentially ramified in and around this region, and it is therefore possible that the widespread collateralization is linked to the multimodal character of the posterior PM. Although our BDA injections did not sample outside this region, the distribution of GAD+PV+ neurons also favors what appears to be the PMm and PMl (Fig. 13).

The physiologically defined dorsomedial pulvinar (Pdm) has been characterized as specialized for selective attentional enhancement of visual responses (Robinson and Cowie, 1997). This zone is shown at the level of the brachium of the superior colliculus (Fig. 2.1G,H in Robinson and Cowie, 1997) and seems to be anterior to the region investigated in the present report. The distribution of GAD+PV+ neurons does, however, extend to this level (Fig. 13C), and a direct relationship might be possible.

Implications for mosaic architecture

Neurochemical studies over the past 10–15 years have successfully defined further subdivisions within the traditional borders of the pulvinar, and for the retinotopically organized inferior pulvinar, these have been correlated with retinotopic maps as well as connectivity patterns. There have been further intriguing observations of a finely organized microarchitecture, namely, patches of heightened staining for cytochrome oxidase or acetylcholinesterase (Lysakowski et al., 1986; Cusick et al., 1993; Cavada et al., 1995; Gutierrez et al., 1995; Stepniewska and Kaas, 1997; Gray et al., 1999), as well as the patchy distribution of corticopulvinar terminations mentioned in the Introduction. It has, however, so far been difficult to define in associational nuclei any connectional and representational units as distinctive as the rod and matrix domains in the primate ventral posterior nuclei (dominated, respectively, by lemniscal and spinothalamic inputs; Rausell and Jones, 1991; Steriade et al., 1997). For the posterior pulvinar, corresponding to the classical PM, it remains unclear whether there is a uniform internal architecture or an architecture consisting of interleaved components.

Cortical connections to the medial pulvinar are generally patchy, and double anterograde injections in paired cortical areas result in variable degrees of overlap, which could be compatible with a modular organization (Gutierrez et al., 2000). Several features of the long-range interneurons are in fact compatible with some kind of modular or mosaic organization, as if these were selectively linking multiple discrete foci. That is, the cell bodies occur either in small clusters or, more commonly, scattered at intervals of about 0.2–0.8 mm, and the axonal ramification, although widespread over an area of about 2.0×1.0 mm^2, consists of multiple terminal foci, each about 1.0 mm or less in length. The 1.0 mm size is in range with many of the terminal foci resulting from large cortical injections. It is, however, larger than individual arbors of type 2 corticopulvinar terminations and less than the widely divergent type 1 axons (Rockland, 1996). Another difference is that terminations of type 1 axons also tend to be more continuously distributed and are higher in number per axon (1,155, 1,280, and 2,456 boutons for three reconstructed axons, Rockland, 1996). Further work, for example, combining double labeling for PC projection foci and GAD+PV+ neurons, might be helpful in clarifying these issues.

There is some evidence of cross-subdivision innervation by corticopulvinar terminations. In the monkey, large cortical injections result in multiple terminal foci, often to separate subdivisions within the pulvinar or even between the pulvinar and mediodorsal nuclei (Romanski et al., 1997), and single axon analysis shows that type 1 corticopulvinar axons can ramify across the full mediolateral extent of the posterior pulvinar, corresponding to at least the PMl and PMm (Figs. 12, 13, and 19 in Rockland, 1996). One such axon has been demonstrated to ramify over 2.5 mm in the anterior-posterior (AP) plane and terminate in parts of the PI as well as the PM (Fig. 12 in Rockland, 1996). The long-range interneurons in the present report seem to be more confined to the vicinity of the PMm and PMl, with an AP extent under 1.0 mm. The GAD+PV+ large neurons also preferentially occur in this posterior region, but the question remains of how these might relate to the internal organization of this region and whether these interneurons ramify within or across adjoining subdivisions in the posterior pulvinar.

ACKNOWLEDGMENTS

We especially thank Ms. Hiromi Mashiko and Ms. Yoshiko Abe for expert technical assistance, Ms. Michiko Fujisawa for assistance with manuscript preparation, and Dr. Noritaka Ichinohe for helpful discussion.

LITERATURE CITED

Adams MM, Hof PR, Gattass R, Webster MJ, Ungerleider LG. 2000. Visual cortical projections and chemoarchitecture of macaque monkey pulvinar. J Comp Neurol 419:377–393.

Arcelli P, Frassoni C, Regondi MC, De Biasi S, Spreafico R. 1997. GABAergic neurons in mammalian thalamus: a marker of thalamic complexity? Brain Res Bull 42:27–37.

Baizer, JS, Desimone R, Ungerleider LG. 1993. Comparison of subcortical connections of inferior temporal and posterior parietal cortex in monkeys. Vis Neurosci 10:59–72.

Baldauf ZB, Chomsung RD, Carden B, May PJ, Bickford ME. 2005a. Ultrastructural analysis of projections to the pulvinar nucleus of the cat. I: Middle suprasylvian gyrus (area 5 and 7). J Comp Neurol 485:87–107.

Baldauf ZB, Wang S, Chomsung RD, May PJ, Bickford ME. 2005b. Ultrastructural analysis of projections to the pulvinar nucleus of the cat. II: Pretectum. J Comp Neurol 485:108–126.

Baleydier C, Mauguiere F. 1987. Network organization of the connectivity between parietal area 7, posterior cingulate cortex and medial pulvinar nucleus: a double fluorescent tracer study in monkey. Exp Brain Res 66:385–393.

Baleydier C, Morel A. 1992. Segregated thalamocortical pathways to inferior parietal and inferotemporal cortex in macaque monkey. Vis Neurosci 8:391–405.

Bartho P, Freund TF, Acsady L. 2002. Selective GABAergic innervation of thalamic nuclei from zona incerta. Eur J Neurosci 16:999–1014.

Basso MA, Uhlrich D, Bickford ME. 2005. Cortical function: a view from the thalamus. Neuron 45:485–488.

Benevento LA, Port JD. 1995. Single neurons with both form/color differential responses and saccade-related responses in the nonretinotopic pulvinar of the behaving macaque monkey. Vis Neurosci 12:523–544.

Bickford ME, Carden WB, Patel NC. 1999. Two types of interneurons in the cat visual thalamus are distinguished by morphology, synaptic connections, and nitric oxide synthase content. J Comp Neurol 413:83–100.

Bokor H, Frere SG, Eyre MD, Slezia A, Ulbert I, Luthi A, Acsady L. 2005. Selective GABAergic control of higher-order thalamic relays. Neuron 45:929–940.

Brandt HM, Apkarian AV. 1992. Biotin-dextran: a sensitive anterograde tracer for neuroanatomic studies in rat and monkey. J Neurosci Methods 45:35–40.

Casanova C, Merabet L, Desautels A, Minville K. 2001. Higher-order motion processing in the pulvinar. Prog Brain Res 134:71–82.

Cavada C, Company T, Hernandez-Gonzalez A, Reinoso-Suarez F. 1995. Acetylcholinesterase histochemistry in the macaque thalamus reveals territories selectively connected to frontal, parietal and temporal association cortices. J Chem Neuroanat 8:245–257.

Celio MR, Baier W, Scharer L, de Viragh P, Gerday C. 1988. Monoclonal antibodies directed against the calcium binding protein parvalbumin. Cell Calcium 9:81–86.

Chalupa LM. 1991. The visual function of the pulvinar. In: Chalupa LM, Werner JS, editors. The visual neurosciences, vol. I. Cambridge: MIT Press. p 592–608.

Clark AS, Schwartz ML, Goldman-Rakic PS. 1989. GABA-immunoreactive neurons in the mediodorsal nucleus of the monkey thalamus. J Chem Neuroanat 2:259–267.

Cola MG, Seltzer B, Preuss TM, Cusick CG. 2005. Neurochemical organization of chimpanzee inferior pulvinar complex. J Comp Neurol 484: 299–312.

Cox CL, Reichova I, Sherman SM. 2003. Functional synaptic contacts by intranuclear axon collaterals of thalamic relay neurons. J Neurosci 23:7642–7646.

Crabtree JW, Isaac JT. 2002. New intrathalamic pathways allowing modality-related and cross-modality switching in the dorsal thalamus. J Neurosci 22:8754–8761.

Cusick CG, Scripter JL, Darensbourg JG, Weber JT. 1993. Chemoarchitectonic subdivisions of the visual pulvinar in monkeys and their connectional relations with the middle temporal and rostral dorsolateral visual areas, MT and DLr. J Comp Neurol 336:1–30.

Darian-Smith C, Tan A, Edwards S. 1999. Comparing thalamocortical and corticothalamic microstructure and spatial reciprocity in the macaque ventral posterolateral nucleus (VPLc) and medial pulvinar. J Comp Neurol 410:211–234.

Gabbott PL, Bacon SJ. 1994. Two types of interneuron in the dorsal lateral geniculate nucleus of the rat: a combined NADPH diaphorase histochemical and GABA immunocytochemical study. J Comp Neurol 350: 281–301.

Gray D, Gutierrez C, Cusick CG. 1999. Neurochemical organization of inferior pulvinar complex in squirrel monkeys and macaques revealed by acetylcholinesterase histochemistry, calbindin and Cat-301 immunostaining, and *Wisteria floribunda* agglutinin binding. J Comp Neurol 409:452–468.

Grieve KL, Acuna C, Cudeiro J. 2000. The primate pulvinar nuclei: vision and action. Trends Neurosci 23:35–39.

Guillery RW. 1995. Anatomical evidence concerning the role of the thalamus in corticocortical communication: a brief review. J Anat 187:583–92.

Guillery RW. 2005. Anatomical pathways that link perception and action. Prog Brain Res 149:235–256

Guillery RW, Feig SL, van Lieshout DP. 2001. Connections of higher order visual relays in the thalamus: a study of corticothalamic pathways in cats. J Comp Neurol 438:66–85.

Gutierrez C, Yaun A, Cusick CG. 1995. Neurochemical subdivisions of the inferior pulvinar in macaque monkeys. J Comp Neurol 363:545–562.

Gutierrez C, Cola MG, Seltzer B, Cusick C. 2000. Neurochemical and connectional organization of the dorsal pulvinar complex in monkeys. J Comp Neurol 419:61–86.

Huang CL, Larue DT, Winer JA. 1999. GABAergic organization of the cat medial geniculate body. J Comp Neurol 415:368–392.

Hunt CA, Pang DZ, Jones EG. 1991. Distribution and density of GABA cells in intralaminar and adjacent nuclei of monkey thalamus. Neuroscience 43:185–196.

Ilinsky IA, Ambardekar AV, Kultas-Ilinsky K. 1999. Organization of projections from the anterior pole of the nucleus reticularis thalami (NRT) to subdivisions of the motor thalamus: light and electron microscopic studies in the rhesus monkey. J Comp Neurol 409:369–384.

Jones EG. 2002. Thalamic organization and function after Cajal. Prog Brain Res 136:333–357.

Jones EG, Hendry SH. 1989. Differential calcium binding protein immunoreactivity distinguishes classes of relay neurons in monkey thalamic nuclei. Eur J Neurosci 1:222–246.

Kultas-Ilinsky K, Fallet C, Verney C. 2004. Development of the human motor-related thalamic nuclei during the first half of gestation, with special emphasis on GABAergic circuits. J Comp Neurol 476:267–289.

Levesque M, Wallman MJ, Parent A. 2004. Striosomes are enriched in glutamic acid decarboxylase in primates. Neurosci Res 50:29–35.

Lysakowski A, Standage GP, Benevento LA. 1986. Histochemical and architectonic differentiation of zones of pretectal and collicular inputs to the pulvinar and dorsal lateral geniculate nuclei in the macaque. J Comp Neurol 250:431–448.

Ma TP, Lynch JC, Donahoe DK, Attallah H, Rafols JA. 1998. Organization of the medial pulvinar nucleus in the macaque. Anat Rec 250:220–237.

Meng XW, Ohara PT, Ralston HJ 3rd. 1996. Nitric oxide synthase immunoreactivity distinguishes a sub-population of GABA-immunoreactive neurons in the ventrobasal complex of the cat. Brain Res 728:111–115.

Mitrofanis J. 2005. Some certainty for the "zone of uncertainty"? Exploring the function of the zona incerta. Neuroscience 130:1–15.

Ogren MP, Hendrickson AE. 1979. The structural organization of the inferior and lateral subdivisions of the *Macaca* monkey pulvinar. J Comp Neurol 188:147–178.

Paxinos G, Huang X-F, Toga AW. 2000. The rhesus monkey brain in stereotaxic coordinates, New York: Academic Press.

Pinault D. 2004. The thalamic reticular nucleus: structure, function and concept. Brain Res Brain Res Rev 46:1–31.

Rausell E, Jones EG. 1991. Histochemical and immunocytochemical compartments of the thalamic VPM nucleus in monkeys and their relationship to the representational map. J Neurosci 11:210–225.

Reiner A, Veeman CL, Medina L, Jiao Y, Ma ND, Honig MG. 2000. Pathway tracing using biotinylated dextran amines. J Neurosci Methods 103:23–37.

Robinson DL, Cowie RJ. 1997. The primate pulvinar: structural, functional, and behavioral components of visual salience. In: Steriade M, Jones EG, McCormick DA, editors. Thalamus: organization and function. Amsterdam: Elsevier. p 53–92.

Rockland KS. 1996. Two types of corticopulvinar terminations: round (type 2) and elongate (type 1). J Comp Neurol 368:57–87.

Romanski LM, Giguere M, Bates JF, Goldman-Rakic PS. 1997. Topo-

graphic organization of medial pulvinar connections with the prefrontal cortex in the rhesus monkey. J Comp Neurol 379:313–332.

Rouiller EM, Welker E. 2000. A comparative analysis of the morphology of corticothalamic projections in mammals. Brain Res Bull 53:727–741.

Scheibel ME, Scheibel AB, Davis TH. 1972. Some substrates for centrifugal control over thalamic cell ensembles. In: Frigyesi TL, Rinvik E, Yahr MD, editors. Corticothalamic projections and sensorimotor activities. New York: Raven Press. p 131–160.

Sherman SM, Guillery RW. 2001. Exploring the thalamus. San Diego: Acadmic Press.

Sherman SM, Guillery RW. 2004. Thalamus. In: Shepherd GM, editor. The synaptic organization of the brain, 5th ed. Oxford: Oxford University Press. p 311–359.

Sherman SM. 2005. Thalamic relays and cortical functioning. Prog Brain Res 149:107–126

Shipp S. 2003. The functional logic of cortico-pulvinar connections. Philos Trans R Soc Lond B Biol Sci 358:1605–1624.

Smith PH, Bartlett EL, Kowalkowski A. 2006. Unique combination of anatomy and physiology in cells of the rat paralaminar thalamic nuclei adjacent to the medial geniculate body. J Comp Neurol 496:314–334.

Smith Y, Seguela P, Parent A. 1987. Distribution of GABA-immunoreactive neurons in the thalamus of the squirrel monkey (*Saimiri sciureus*). Neuroscience 22:579–591.

Soares JG, Gattass R, Souza AP, Rosa MG, Fiorani M Jr, Brandao BL. 2001. Connectional and neurochemical subdivisions of the pulvinar in Cebus monkeys. Vis Neurosci 18:25–41.

Stepniewska I. 2004. The pulvinar complex. In: Kaas JH, Collins CE, editors. The primate visual system. Boca Raton: CRC Press. p 53–80.

Stepniewska I, Kaas JH. 1997. Architectonic subdivisions of the inferior pulvinar in New World and Old World monkeys.Vis Neurosci 14:1043–1060.

Steriade M, Jones EG, McCormick DA. 1997. Organisation and function, vol. I. Amsterdam: Elsevier.

Taktakishvili O, Sivan-Loukianova S, Kultas-Illinsky K, Illinsky IA. 2002. Posterior parietal cortex projections to the ventral lateral and some association thalamic nuclei in *Macaca mulatta*. Brain Res Bull 59:135–150.

Tokuno H, Hatanaka N, Chiken S, Ishizuka N. 2002. An improved method with a long-shanked glass micropipette and ultrasonography for drug injection into deep brain structure of the monkey. Brain Res Brain Res Protoc 10:16–22.

Tombol T. 1969. Two types of short axon (Golgi 2nd) interneurons in the specific thalamic nuclei. Acta Morphol Acad Sci Hung 17:285–297.

Trageser JC, Keller A. 2004. Reducing the uncertainty: gating of peripheral inputs by zona incerta. J Neurosci 24:8911–8915.

Veenman CL, Reiner A, Honig MG. 1992. Biotinylated dextran amine as an anterograde tracer for single- and double-labeling studies. J Neurosci Methods 41:239–254.

Vercelli A, Repici M, Garbossa D, Grimaldi A. 2000. Recent techniques for tracing pathways in the central nervous system of developing and adult mammals. Brain Res Bull 51:11–28.